CHEMISTRY OF MATERIALS

Article

pubs.acs.org/cm

Open-Circuit Voltage Losses in Selenium-Substituted Organic Photovoltaic Devices from Increased Density of Charge-Transfer States

Dana B. Sulas,[†,§] Kai Yao,[‡,§,∇] Jeremy J. Intemann,[‡,⊥] Spencer T. Williams,[‡] Chang-Zhi Li,[‡,¶] Chu-Chen Chueh,[‡] Jeffrey J. Richards,[#] Yuyin Xi,[#] Lilo D. Pozzo,[#] Cody W. Schlenker,*[,†] Alex K.-Y. Jen,*[,‡] and David S. Ginger*[,†]

[†]Department of Chemistry, [‡]Department of Materials Science and Engineering, and [#]Department of Chemical Engineering, University of Washington, Seattle, Washington 98195, United States

Supporting Information

ABSTRACT: Using an analysis based on Marcus theory, we characterize losses in open-circuit voltage (V_{OC}) due to changes in charge-transfer state energy, electronic coupling, and spatial density of charge-transfer states in a series of polymer/fullerene solar cells. We use a series of indacenodithiophene polymers and their selenium-substituted analogs as electron donor materials and fullerenes as the acceptors. By combining device measurements and spectroscopic studies (including subgap photocurrent, electroluminescence, and, importantly, time-resolved photoluminescence of the charge-transfer state) we are able to isolate the values for electronic coupling and the density of charge-transfer states (N_{CT}), rather than the more commonly measured product of these values. We find values for N_{CT} that are surprisingly large (~4.5×10^{21}–6.2×10^{22} cm^{-3}), and we find that a significant increase in N_{CT} upon selenium substitution in donor polymers correlates with lower V_{OC} for bulk heterojunction photovoltaic devices. The increase in N_{CT} upon selenium substitution is also consistent with nanoscale morphological characterization. Using transmission electron microscopy, selected area electron diffraction, and grazing incidence wide-angle X-ray scattering, we find evidence of more intermixed polymer and fullerene domains in the selenophene blends, which have higher densities of polymer/fullerene interfacial charge-transfer states. Our results provide an important step toward understanding the spatial nature of charge-transfer states and their effect on the open-circuit voltage of polymer/fullerene solar cells.

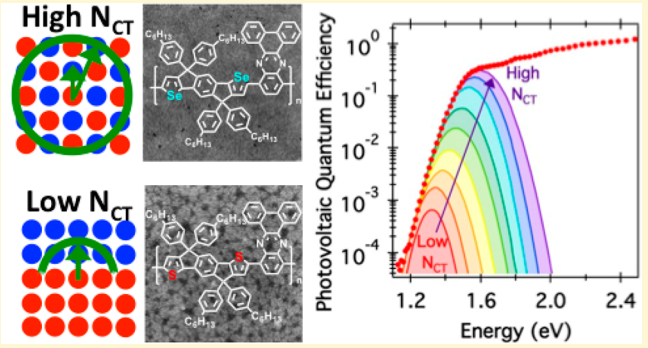

INTRODUCTION

Organic photovoltaics (OPVs) have the potential to reduce the costs and environmental impacts associated with power generation by serving as lightweight, flexible, and easily processed solar power conversion devices made from abundant and nontoxic materials. OPV power conversion efficiencies (PCEs) have been steadily increasing, with a number of materials exhibiting efficiencies in the 7−10% range.[1−4] Nevertheless, many calculations indicate that OPVs should be able to reach much higher efficiencies, suggesting substantial room for improvement if one can understand the factors that limit device performance.[5,6]

The general path toward higher efficiency OPVs seems straightforward: it involves harvesting a broader range of the solar spectrum with lower band gap materials while maintaining energetic landscapes that favor exciton dissociation.[7] The task is complicated by the need to simultaneously optimize donor/acceptor phase morphology for efficient charge transport[8,9] as well as suppress recombination losses both in the bulk[10−12] and at electrode interfaces.[13−15] Despite significant progress in this field, successful strategies to achieve these goals remain elusive and, in many cases, depend on a deeper understanding of the mechanisms underpinning the loss processes.

The highest efficiency OPVs at present are bulk heterojunction (BHJ) cells that make use of photoinduced charge transfer between electron donor (typically a conjugated polymer) and electron acceptor (often a fullerene derivative) materials. Numerous reports have identified the formation of charge-transfer (CT) states at the polymer/fullerene interface in these blends, which can be excited directly with light or formed by recombination of electron−hole pairs.[16−20] While spectroscopic evidence of the charge-transfer state is observed in most polymer/fullerene blends, its spatial form and role in charge separation are still debated. Some studies have proposed that successful photocurrent generation likely bypasses the charge-transfer state in favor of direct free charge formation

Received: June 6, 2015
Revised: August 23, 2015
Published: August 24, 2015

DOI: 10.1021/acs.chemmater.5b02133
Chem. Mater. 2015, 27, 6583−6591

across the donor/acceptor interface,[21,22] but others report that charge generation via the lowest energy charge-transfer state proceeds with high efficiency.[16,23] Regardless of whether the charge-transfer state is a key intermediate for charge formation, whether it is a trap state that mediates charge carrier recombination, or both, there is a large body of empirical evidence (such as the relationship between open-circuit voltage and charge-transfer state energy) indicating that charge-transfer state properties correlate with device performance.[12,24−26]

Many studies have concluded that charge carrier recombination via the charge-transfer state limits open-circuit voltage (V_{OC}).[12,17,26−29] Initially, the energy of the excited charge-transfer state (E_{CT}) and the electronic coupling between the initial and final states of charge transfer were thought to dominate recombination losses.[17,26−28] However, more recent work has gone beyond the role of energetics to study the spatial density of recombination centers.[12] For instance, Vandewal and co-workers studied the effects of donor/acceptor interfacial area, showing that a reduction in the spatial density of charge-transfer states (N_{CT}) could lead to increased V_{OC}.[29] However, most studies have not reported measurements of N_{CT} because the most common experimental probes measure the product of N_{CT} and donor/acceptor electronic coupling.[26] Even those studies that report qualitative changes in N_{CT} have done so in systems with low donor/acceptor ratios and by the implicit assumption that under specific film fabrication conditions the degree of electronic coupling will remain invariant, allowing the authors to attribute variations in subgap photocurrent to variations in N_{CT}.[29]

Here, we investigate V_{OC} losses in organic photovoltaic devices made from selenium-substituted polymer donors blended with fullerene acceptors. We individually evaluate the effects of charge-transfer state energy, spatial density of charge-transfer states, and electronic coupling between the ground-state polymer/fullerene complex and excited CT state. We find that N_{CT} and electronic coupling both increase upon Se substitution, but the increase in N_{CT} is more substantial and has a significant impact on V_{OC}. The increase in N_{CT} that we calculate from device performance is consistent with the more intermixed polymer/fullerene morphology that we observe by electron microscopy and electron diffraction.

RESULTS AND DISCUSSION

Scheme 1 shows the series of four structurally similar polymers that we studied. The polymers are distinguished by varying either the selenium substitution on the indacenodithiophene unit or by aromatic ring fusion of the diphenyl substituents of the quinoxaline. We synthesized PIDT-PhanQ and PIDT-PhQ following previous reports[30] and prepared PIDSe-PhanQ and PIDSe-PhQ via Stille coupling. The detailed synthetic methods and structural characterization are given in the Supporting Information. Figure S1 shows UV−vis spectra of the polymers, confirming that Se-atom substitution leads to a lower energy onset of the thin film absorption spectrum corresponding to a lower optical band gap of 1.53 eV for PIDSe-PhanQ compared to 1.70 eV for PIDT-PhanQ and 1.65 eV for PIDSe-PhQ compared to 1.79 eV for PIDT-PhQ. This decrease in band gap upon Se substitution for S on the indacenodithiophene ring is consistent with previous reports and is generally attributed to a lower LUMO energy arising from increased Se atom polarizibility compared to S.[31] Table S1 summarizes the UV−vis absorption and cyclic voltammetry data confirming a drop in band gap energy for both Se-substituted polymers corresponding mainly to a change in reduction potential (LUMO position).

Scheme 1. Molecular Structures of the Donor Polymers and Acceptor Fullerene Used in This Study

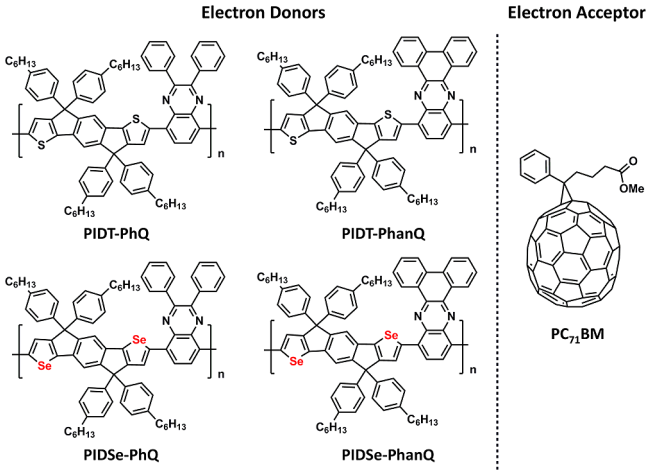

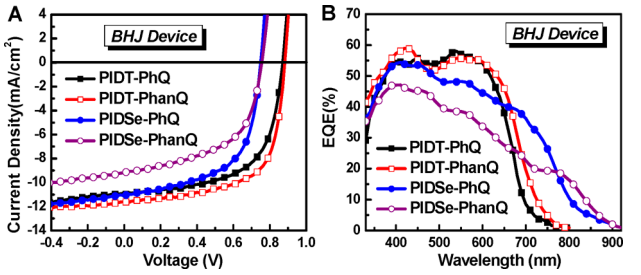

Figure 1. a) Current−voltage curves taken under 1 sun illumination and b) photovoltaic external quantum efficiency (EQE_{PV}). The current−voltages curves show a large open-circuit voltage (V_{OC}) drop upon selenium substitution in the donor polymer when the donor and acceptor materials are intimately mixed in the bulk heterojunction (BHJ) device configuration.

Table 1. Short-Circuit Current Density (J_{sc}), Open-Circuit Voltage (V_{OC}), Fill Factor (FF), and Power Conversion Efficiency (PCE) for Bulk Heterojunction Polymer/Fullerene Devices under 1 Sun Illumination

active layer	J_{sc} (mA cm^{-2})	V_{oc} (V)	FF	PCE (%)[a]
PIDSe-PhanQ:$PC_{71}BM$	9.16 ± 0.17	0.75 ± 0.01	0.57 ± 0.02	3.93 ± 0.18
PIDT-PhanQ:$PC_{71}BM$	11.61 ± 0.18	0.88 ± 0.01	0.65 ± 0.02	6.63 ± 0.22
PIDSe-PhQ:$PC_{71}BM$	11.04 ± 0.22	0.75 ± 0.01	0.59 ± 0.02	4.89 ± 0.20
PIDT-PhQ:$PC_{71}BM$	10.86 ± 0.20	0.87 ± 0.01	0.62 ± 0.02	5.91 ± 0.24

[a]Error values represent the standard deviation of the mean of 20 devices.

We study the effect of these small variations in polymer structure on photovoltaic device performance. Figure 1 and Table 1 summarize the photovoltaic external quantum efficiencies (EQE_{PV}), current−voltage (JV) characteristics, and power conversion efficiency (PCE) averaged over 20 devices of each type for the four polymers in bulk

DOI: 10.1021/acs.chemmater.5b02133
Chem. Mater. 2015, 27, 6583−6591

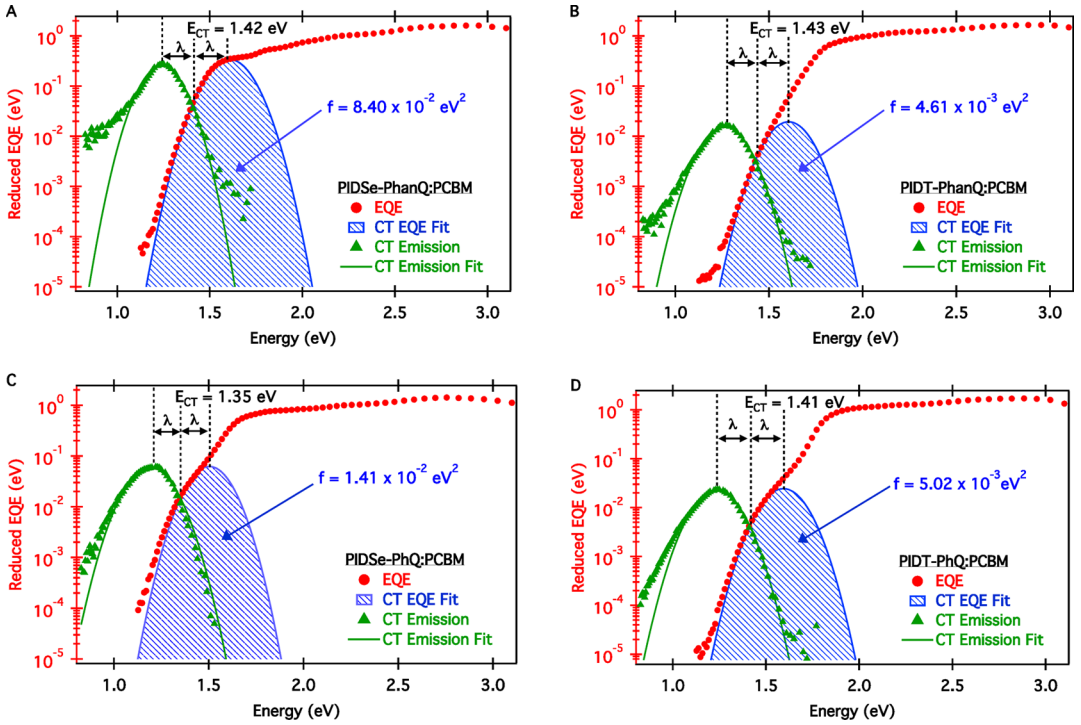

Figure 2. Reduced external quantum efficiencies (EQE) (red circles) and scaled electroluminescence spectra for bulk heterojunction devices of a) PIDSe-PhanQ:PCBM, b) PIDT-PhanQ:PCBM, c) PIDSe-PhQ:PCBM, and d) PIDT-PhQ:PCBM showing charge-transfer state absorption fit by eq 2a and demonstrating increased charge-transfer state absorption intensity and coupling constant (f) value for Se-substituted devices. Fits of electroluminescence spectra (green triangles) are used to constrain the charge-transfer state energy (E_{CT}) and reorganization energy (λ) during the charge-transfer state absorption fit. Electroluminescence spectra are scaled to the height of the respective CT absorption band in order to emphasize the definitions of E_{CT} and λ.

heterojunction (BHJ) device structures. We observe lower overall efficiency along with a significant open-circuit voltage (V_{OC}) loss of 120−130 mV upon Se substitution. Figure 1b also shows red-shifted photocurrent generation in Se-substituted devices. While this red-shift is partly due to the lower band gap in the Se-substituted polymers, Figure S3 shows that the absorption features in the BHJ blends extend to even lower energies than the onset of the neat materials' absorption. We attribute this low-energy absorption feature to direct excitation from the neutral ground state to the excited charge-transfer state.

Since the energy,[17] number density,[12,29] and electronic coupling[26,28] of charge-transfer states have all been linked to V_{OC}, we next explore the relative importance of these parameters in explaining the 120−130 mV lower V_{OC} of selenophene versus thiophene polymers in the bulk heterojunction devices.

Based on the electroluminescence spectra of the charge-transfer state and the subgap EQE_{PV} spectra (Figure 2), we determine that the energies of the charge-transfer states are similar within ∼10 meV for PhanQ systems irrespective of Se substitution, suggesting that the 130 mV drop in V_{OC} cannot be explained by a change in charge-transfer state energy in the PhanQ blends. We find that the charge-transfer state energy changes by about 60 meV upon Se substitution in PhQ systems, which may account for up to ∼50% of the V_{OC} drop in the PhQ blends. In both cases, more than energetics must be responsible for the lower V_{OC} upon Se substitution.

Figure 2 shows the lock-in detected EQE_{PV} and normalized charge-transfer state electroluminescence spectra that we use to extract the charge-transfer state energies and quantify the voltage deficit, defined as $q^{-1}E_{CT} - V_{OC}$,[12] for each BHJ device (where q is the elementary charge).[17] We observe infrared charge-transfer state emission at similar energies and peak widths commonly measured for polymer/fullerene blends.[19] The peak electroluminescence intensity occurs near the EQE_{PV} onset, as is expected for charge-transfer state emission.[32] We observe a distinct shoulder in the low energy portion of the EQE_{PV} spectrum for PhQ blends and a steeper low energy EQE_{PV} drop off in PhanQ blends. The energy difference of ∼350 meV between the EQE_{PV} shoulder, and the peak electroluminescence intensity is consistent with Stokes shifts previously reported for charge-transfer states in polymer/fullerene blends.[33]

We extract the charge-transfer state energy and reorganization energy (λ) by fitting *both* the charge-transfer state electroluminescence and EQE_{PV}. Literature reports commonly find E_{CT} and λ by fitting the low energy portion of the EQE_{PV} spectrum,[25,26,29,34] though a smaller number of studies report simultaneous fits of both data sets.[17,33] To reduce the error associated with fitting only part of the Gaussian curve in the charge-transfer state absorption region of EQE_{PV}, we first constrain the sum $E_{CT} + \lambda$ by fitting the electroluminescence spectrum according to the reduced equation for the charge-transfer state radiative decay rate (I_{rad}) derived from Marcus theory (eqs 1a and 1b).[35,36] Using these constrained values, we then fit the low energy portion of the EQE_{PV} spectrum with the reduced equation for photocurrent generation from direct excitation of the charge-transfer complex (eqs 2a and 2b).[17] We provide a detailed explanation of our fitting procedure in Section 3.1 of the Supporting Information.

DOI: 10.1021/acs.chemmater.5b02133
Chem. Mater. 2015, 27, 6583−6591

$$\frac{I_{rad}(E)}{E} = \frac{f_{emission}}{\sqrt{4\pi\lambda kT}} \exp\left(\frac{-(E_{CT} - \lambda - E)^2}{4\lambda kT}\right) \quad (1a)$$

$$f_{emission} = \frac{64\pi^4}{3h^4c^3} n^3 V^2 \Delta\mu^2 \left[6.24*10^{-25} \frac{eV\ cm^3}{D^2}\right] \quad (1b)$$

$$EQE_{PV}(E)E = \frac{f}{\sqrt{4\pi\lambda kT}} \exp\left(\frac{-(E_{CT} + \lambda - E)^2}{4\lambda kT}\right) \quad (2a)$$

$$f = \eta N_{CT} 2d \frac{8\pi^3}{3hc} n V^2 \Delta\mu^2 \left[6.24*10^{-25} \frac{eV\ cm^3}{D^2}\right] \quad (2b)$$

In eqs 1a−2b, E is the photon energy [eV], k is Boltzmann's constant [eV K^{-1}], T is temperature [K], λ is the reorganization energy [eV], E_{CT} is the excited CT state energy [eV], $f_{emission}$ is the coupling constant associated with the emission process [eV^{-1} s^{-1}],[17] f is the coupling constant associated with the absorption process [eV^2],[17] h is Planck's constant [eV s], c is the speed of light [cm s^{-1}], n is the refractive index, η is the internal photon to electron conversion efficiency, N_{CT} is the total density of available charge-transfer states [cm^{-3}], d is the film thickness [cm], V is the electronic coupling matrix element [eV] between the initial and final states of electron transfer (i.e., the neutral ground state and CT exciton), and $\Delta\mu$ is the difference in dipole moment between the initial and final states of electron transfer [D]. Section 4.1 in the Supporting Information gives an explanation of the unit conversion included in eqs 1b and 2b.

Popularized by Vandewal and co-workers, the Marcus formalism is currently widely used to characterize charge-transfer state properties in polymer/fullerene blends.[12,17,25,26,29,34] While there is general agreement that the subgap absorption features are associated with interfacial charge-transfer states, the width of these features also likely has contributions from energetic disorder in the band tails.[37−39] While a deeper comparison of the available models is beyond the scope of the current discussion, we note that the effect of disorder can be represented in analyses based on eqs 1a−2b as fixed deviations in E_{CT} and λ from the ideal case.[12] In other words, increased disorder lowers the E_{CT} extracted from a Marcus analysis, having the effect of reducing the expected V_{OC}. It should therefore be noted that, under the current model, changes in E_{CT} upon Se substitution represent a combined change in E_{CT} and disorder. However, our main conclusions are unaffected by our use of the classic formalism rather than separately extracting disorder, since our analysis focuses on cases where changes in V_{OC} cannot be accounted for solely by changes in the experimentally measured E_{CT} (which folds in changes in disorder).

Figure 2 gives the values of E_{CT} for each BHJ device. The fits indicate that PIDT-PhQ, PIDSe-PhanQ, and PIDT-PhanQ BHJ devices all have similar charge-transfer state energies (1.41, 1.42, and 1.43 eV, respectively), while the PIDSe-PhQ BHJ device has a lower charge-transfer state energy (1.35 eV). However, both Se-substituted devices have a higher voltage deficit ($q^{-1}E_{CT} - V_{OC}$) compared to their thiophene counterparts, indicative of larger recombination losses. Most notably, PIDSe-PhanQ has a significantly larger V_{OC} loss than the other three devices, despite having a charge-transfer state energy comparable to the thiophene devices. We next turn to investigate the origin of the increased recombination in the selenophene systems, especially the PIDSe-PhanQ blend.

Though previous reports have identified both electronic coupling[28] and spatial density of charge-transfer states[12,29] as possible factors affecting recombination losses, few studies are able to separately measure these values.[26] Most studies rely on coupling constant (f) values, which contain the product of electronic coupling with the spatial density of charge-transfer states (see eq 2b).[17,26,29,40] A few experimental[28] and computational[41−43] studies have estimated values for electronic coupling, and only one study to our knowledge has determined a range of possible values for the spatial density of charge-transfer states.[12] We therefore present a comprehensive experimental study using the coupling constant to quantitatively assess the magnitudes of charge-transfer state density and electronic coupling as well as their effects on the open-circuit voltage.

We calculate the coupling constant using two separate approaches, and we find that both give increased coupling constant values for the Se-containing blends. First, we obtain coupling constant values from the EQE_{PV} fits to eq 2a, and we give the results in Figure 2.[17] Consistent with the increased recombination losses measured in the selenophene devices, we extract a larger coupling constant value for Se-substituted BHJ blends, with a ∼2× increase (from 5.02×10^{-3} eV^2 to 1.41×10^{-2} eV^2) in PhQ systems and a nearly ∼20× increase (from 4.61×10^{-3} eV^2 to 8.40×10^{-2} eV^2) in the PhanQ systems. We also apply a second approach to calculate the coupling constants by using the voltage deficit ($q^{-1}E_{CT} - V_{OC}$) along with the charge-transfer state electroluminescence quantum yield, as outlined by Vandewal et al.[17] Using this approach (see Section 3.4 of the Supporting Information), we obtain similar trends, confirming that these values increase upon Se substitution whether determined from photovoltaic EQE or electroluminescence quantum yield data.

While the coupling constant value depends on both electronic ($V\Delta\mu$) and spatial (N_{CT}) molecular interactions, we next show that the higher coupling constant upon Se substitution mainly results from increased N_{CT}. Based on the charge-transfer state photoluminescence lifetime and photoluminescence quantum yield, we separate the effects of electronic coupling and N_{CT}, and we conclude that a significant portion of V_{OC} loss upon Se substitution is due to increased spatial density of charge-transfer states, while electronic coupling plays a smaller role.

Figures 3b and 3d show the photoluminescence spectra for each BHJ blend. We observe two photoluminescence peaks near 1.25 and 1.70 eV. As is commonly observed in OPV blends, we find that the photoluminescence signatures of the individual donor/acceptor components are highly quenched in all blends, though not completely eliminated.[19,44] The peak near 1.25 eV closely matches the charge-transfer state emission peak measured by electroluminescence (Figures S7−S10), and the peak near 1.70 eV corresponds to unquenched emission from the neat materials (Figure S2). We measure the photoluminescence spectra using lock-in techniques, and we find that the photoluminescence quantum yield of the charge-transfer state is around 100 times lower than that of the neat polymer. We observe similar luminescence intensities for all BHJ films with no clear trend in photoluminescence quantum yield upon Se substitution.

We measure time-resolved photoluminescence decays for both the charge-transfer state (Figures 3a and 3c) and the

DOI: 10.1021/acs.chemmater.5b02133
Chem. Mater. 2015, 27, 6583−6591

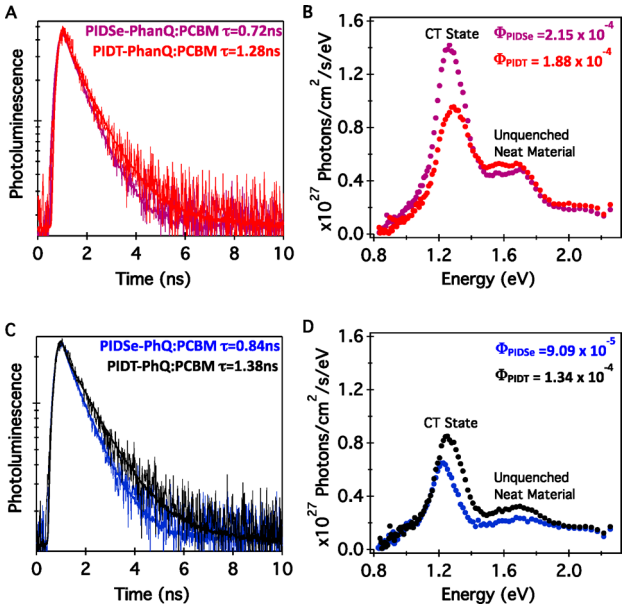

Figure 3. Normalized time-resolved photoluminescence of the charge-transfer state for a) PIDSe-PhanQ:PCBM and PIDT-PhanQ:PCBM and c) PIDSe-PhQ:PCBM and PIDT-PhQ:PCBM with lifetimes extracted from a monoexponential decay fit. The charge-transfer state photoluminescence quantum yields for b) PIDSe-PhanQ:PCBM and PIDT-PhanQ:PCBM and d) PIDSe PIDSe-PhQ:PCBM and PIDT-PhQ:PCBM estimated by the relative intensity of the 1.24 eV peak. Combining lifetimes and photoluminescence quantum yield in eq 3 gives a slightly faster radiative charge-transfer state lifetime for Se-substituted blends.

unquenched neat materials (Figure S13). Figures 3a and 3c show normalized photoluminescence decays probed at energies below 1.18 eV, which exhibit monoexponential decays with nanosecond-scale lifetimes. These lifetimes are similar to previously reported results for polymer/fullerene charge-transfer states, which range from 0.4–6.8 ns.[12,43−47] The single-exponential fits (performed as reconvolution fits of a single-exponential with the instrument response function, see Section 7.1 of the Supporting Information) yield faster photoluminescence decays for Se-substituted blends, corresponding to a faster total charge-transfer state lifetime including both radiative and nonradiative processes. Figure S13 shows the photoluminescence decays of the unquenched neat materials probed at 1.77 eV, which are distinct from the charge-transfer state lifetime.

Eqs 1a and 1b show that the rate of charge-transfer state emission depends on electronic coupling but not the spatial density of charge-transfer states. Measuring the rate of charge-transfer state emission therefore allows us to isolate variations in electronic coupling from the spatial density of charge-transfer states and obtain numeric values for both variables. Integrating eq 1a with respect to energy gives the rate constant for radiative charge-transfer state decay (k_{rad}), which we experimentally quantify using the charge-transfer state lifetime (τ) and the photoluminescence quantum yield (Φ_{rad}).[36]

$$k_{rad} = \frac{64\pi^4}{3h^4c^3} n^3 V^2 \Delta\mu^2 E_{rad} \left[6.24{*}10^{-25} \frac{\text{eV cm}^3}{D^2}\right] = \frac{\Phi_{rad}}{\tau} \quad (3)$$

In eq 3, E_{rad} is the average emission energy [eV], and $\Delta\mu$ is approximated as 15 D for all blends (see Section 5.1 of the Supporting Information).

We summarize the electronic coupling values in Table 2 and find that electronic coupling does increase slightly upon Se

Table 2. Values for Electronic Coupling (V) and Spatial Density of Charge-Transfer States (N_{CT}) As Determined by Time-Resolved Photoluminescence and EQE$_{PV}$ Measurements

	N_{CT} ($\times 10^{21}$ cm^{-3})	electronic coupling, V (meV)
PIDSe-PhanQ:PCBM	62 ± 27	30 ± 6
PIDT-PhanQ:PCBM	4.5 ± 1.8	21 ± 4
PIDSe-PhQ:PCBM	19 ± 9.8	19 ± 5
PIDT-PhQ:PCBM	5.8 ± 4.3	17 ± 6

substitution. However, the increase in electronic coupling could only account for a small portion of the observed V_{OC} loss if N_{CT} were to remain constant. We estimate that this slight increase in electronic coupling would account for 14 ± 3.0% of the 130 mV V_{OC} decrease upon Se substitution in PhanQ blends and 4.6 ± 1.4% of the 120 mV V_{OC} decrease in PhQ blends (see discussion in Section 6.1 of the Supporting Information).

We find that increased N_{CT} is responsible for a larger portion of V_{OC} loss. By inserting our measured V and f values into eq 2b, we find that N_{CT} is tripled upon Se substitution in PhQ blends and increases by over an order of magnitude upon Se substitution in PhanQ blends (values given in Table 2). This substantial increase in N_{CT} would account for 52 ± 20% of the 130 mV V_{OC} decrease upon Se substitution in PhanQ blends and 29 ± 11% of the 120 mV V_{OC} decrease in PhQ blends (see discussion in Section 6.1 of the Supporting Information). The remaining V_{OC} loss is primarily due to the decrease in charge-transfer state energy and the decrease in electroluminescence quantum yield.

We note that the N_{CT} values in Table 2 are large compared to the expected fullerene density in the film (~10^{21} molecules cm^{-3}). However, it is important to distinguish that N_{CT} corresponds to the total density of available charge-transfer states (i.e., the total number of possible donor–acceptor interactions), not the density of simultaneously occupied charge-transfer states.[12] Therefore, the results suggest that ~5–60 fullerene states may be spatially accessible to each polymer donor unit.[12] While it seems surprising that N_{CT} could be ~5–60 times larger than the molecular density, Burke et al. similarly concluded that ~32 CT states per molecule were necessary to account for common $q^{-1}E_{CT} - V_{OC}$ deficits,[12] and Street et al. estimated that electronic states may be delocalized over 20–30 molecules in polymer/fullerene blends.[38] The consistency between these separate results might imply a manifold of charge-transfer states involving donor/acceptor interactions beyond the nearest-neighbor pairs.[12] This further implies that even molecules not directly located at a heterojunction may participate in a charge-transfer state. Though the values are high, we note that these N_{CT} values are comparable to densities of states in inorganic materials with delocalized band structures, which range from 10^{19}–10^{23} cm^{-3}.[48−51] While we take our results to be in experimental agreement with the analysis of Burke et al., we believe that future work is needed to evaluate the origin of these high N_{CT} densities in organic systems in more detail.

DOI: 10.1021/acs.chemmater.5b02133
Chem. Mater. 2015, 27, 6583–6591

Finally, we turn to speculate on a possible cause for the higher N_{CT} values for the selenophene blends. Several reports imply that the degree of molecular mixing as well as the interaction range between donor/acceptor pairs may both contribute to N_{CT}.[12,24,52,53] Figure 4 depicts this relationship

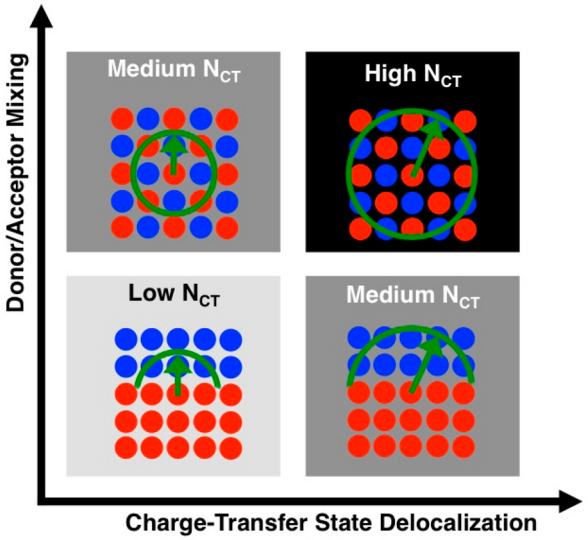

Figure 4. Schematic representation of a possible relationship between donor/acceptor morphology and charge-transfer state density (N_{CT}). We propose that N_{CT} may increase due to more intimate donor/acceptor mixing, increased charge-transfer state delocalization, or both.

schematically. The green arrow represents a possible charge-transfer complex, which forms between a donor/acceptor pair. N_{CT} may increase when donor/acceptor molecules are more intimately mixed, because a given donor molecule would have access to more acceptor molecules within the CT delocalization area and vice versa. N_{CT} may also increase if the degree of molecular mixing does not change, but the charge-transfer state is delocalized over a larger area. One possible cause of CT state delocalization is increased crystallinity.[34] Although carrier delocalization in organic electronics is generally viewed as beneficial,[11,22] if both molecular mixing and CT state delocalization increase simultaneously, we may expect N_{CT} to be relatively high. This speculative hypothesis is qualitatively consistent with our morphological studies on the polymer/fullerene BHJ blends, which we present below.

Figure 5 shows bright field transmission electron microscopy (TEM) images for the BHJ blends as well as the selected area electron diffraction (SAED) patterns with a comparison of the SAED radial intensity profiles. The TEM images show 10−100 nm scale phase regions in the thiophene blends. We do not observe phase segregation on this scale in the selenophene blends, despite the higher Z-contrast of Se compared to S. This result suggests that there is finer donor/acceptor mixing in the selenophene blends. Increased mixing upon Se substitution would be consistent with the higher N_{CT} values that we observe and would place the selenophene blends on the upper portion of our cartoon in Figure 4 compared to the thiophene blends.

Figure 5 also shows a sharp diffraction ring at Q = 0.613 nm^{-1} (1.63 nm) for the PIDSe-PhanQ:PCBM blend, the BHJ with the largest voltage deficit and largest N_{CT} value. The diffraction ring indicates a highly ordered feature. It is important to note that the ring is not present in the radial profiles for either neat PIDSe-PhanQ or neat fullerene. The

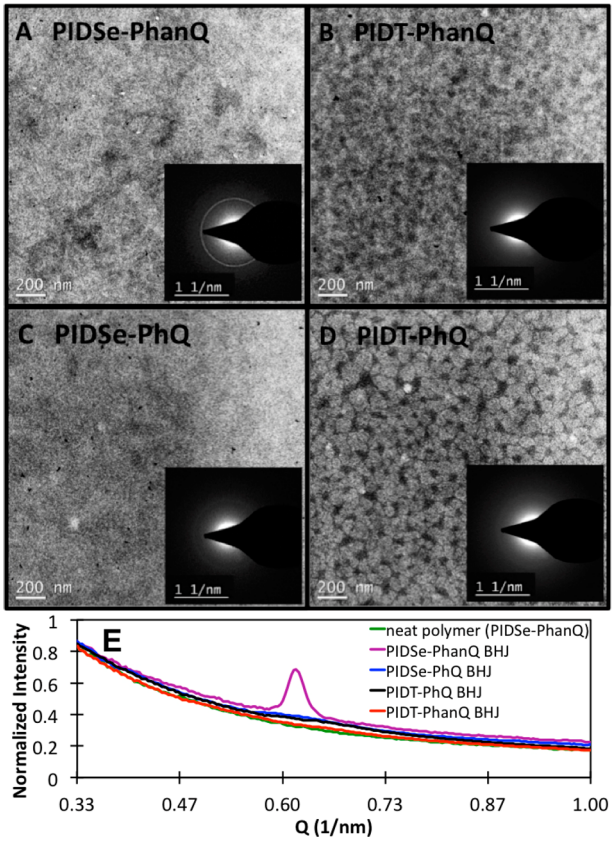

Figure 5. Transmission electron microscopy images and selected area electron diffraction profiles for a) PIDSe-PhanQ:PCBM, b) PIDT-PhanQ:PCBM, c) PIDSe-PhQ:PCBM, and d) PIDT-PhQ:PCBM showing reduced phase separation in Se-substituted blends and a higher degree of fullerene-induced crystallization for the PIDSe-PhanQ:PCBM blend; e) radial intensity profile of SAED images, showing a sharp diffraction peak for PIDSe-PhanQ BHJ.

diffraction ring is entirely absent in the PIDT-PhanQ:PCBM blend, and both the PIDSe-PhQ:PCBM and the PIDT-PhQ:PCBM blends show only a weak signal near Q = 0.59−0.73 nm^{-1} (1.7−1.4 nm). This sharp diffraction ring in the PIDSe-PhanQ BHJ indicates that there is some molecular ordering in this system that is mostly absent in the other BHJ blends and entirely absent in the neat materials. We confirm the presence of this uniquely ordered feature in the PIDSe-PhanQ:PCBM blend using grazing incidence wide-angle X-ray scattering (GIWAXS) experiments (discussed in Section 8.1 of the Supporting Information). We may interpret the highly ordered feature as a polymer/fullerene cocrystalline structure or as polymer packing induced by the presence of fullerene.[53−55] The increase in molecular ordering may place the PIDSe-PhanQ:PCBM blend on the right side of our cartoon in Figure 4 and would be consistent with the increased N_{CT} value that we observe.

Taken together, we find that disrupted phase separation upon Se substitution and a fullerene-induced crystalline feature in the PIDSe-PhanQ BHJ blend are suggestive that N_{CT} may qualitatively correlate with thin-film morphology as depicted in Figure 4 and that rational morphological control of N_{CT} may be a viable route to reduce V_{OC} loss. Indeed, Figure 6 shows that the Se-induced voltage deficit is substantially reduced in planar heterojunction devices with intentionally suppressed donor/acceptor mixing.

DOI: 10.1021/acs.chemmater.5b02133
Chem. Mater. 2015, 27, 6583−6591

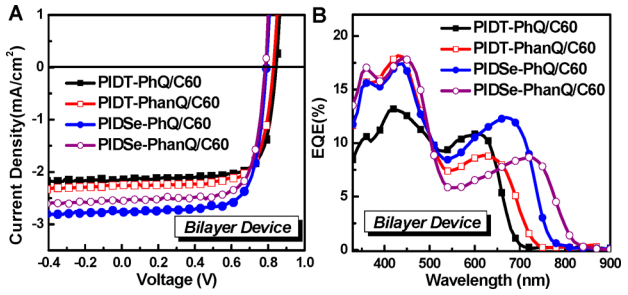

Figure 6. Bilayer device measurements, including a) current−voltage curves taken under 1 sun illumination and b) photovoltaic external quantum yield (EQE_{PV}). The current−voltage curves show a minimal open-circuit voltage (V_{OC}) drop upon selenium substitution in the donor polymer when the interfacial area between the donor and acceptor materials is minimized in the bilayer device configuration.

Figure 6 shows the current−voltage curves and EQE_{PV} for bilayer device structures, which must have reduced donor/acceptor interface area compared to the BHJ blends. We observe reduced EQE_{PV} signal from direct CT state absorption as well as a 30−40 mV drop in V_{OC} upon Se substitution for bilayer devices, which is significantly smaller than the 120−130 mV drop that we observe for the bulk heterojunction blends (Figure 1). The reduced voltage deficit in bilayer devices would be consistent with lower N_{CT} compared to the BHJ blends.

CONCLUSION

We present a unique separation of the contributions of electronic coupling and density of charge-transfer states to open-circuit voltage losses in a series of polymer/fullerene blends. After evaluating a number of device and spectroscopic properties, our data suggest that increased recombination in Se-substituted devices leading to V_{OC} loss is strongly affected by a higher spatial density of charge-transfer states (N_{CT}). We first find the product of electronic coupling and N_{CT} by fitting the low energy portion of the EQE_{PV} spectrum. We show that this product increases for blends with higher V_{OC} loss. We then separate this product into electronic coupling and N_{CT} by measuring CT state photoluminescence lifetime and quantum yield. Using the time-resolved photoluminescence decays for charge-transfer state emission, we find that electronic coupling does increase upon Se substitution but that a larger portion of the experimental V_{OC} loss is attributable to increased N_{CT}. Consistent with a recently published proposal,[12] the N_{CT} values extracted from our analysis (4.51×10^{21}−6.22×10^{22} cm^{-3}) seem uncomfortably large for a weakly interacting molecular system. To explain this discrepancy, we finally take the liberty to speculate on the spatial nature of charge-transfer states by correlating high N_{CT} values with intermixed morphology *and* fullerene-induced crystallization in the selenophene BHJ blends. Our work implies that both electronic coupling and N_{CT} are tunable with small changes in molecular structure, and it implies that controlling these parameters is a route to intelligent molecular design for higher efficiency OPV devices. Future studies may find fruitful ground in focusing on understanding the relationship between N_{CT} and thin-film morphology in more detail.

ASSOCIATED CONTENT

Supporting Information

The Supporting Information is available free of charge on the ACS Publications website at DOI: 10.1021/acs.chemmater.5b02133.

Experimental methods, additional spectra, polymer characteristics, film thicknesses, unit conversions, coupling constant calculations, and relative contribution of V and N_{CT} calculations (PDF)

AUTHOR INFORMATION

Corresponding Authors

*E-mail: ginger@chem.washington.edu.
*E-mail: schlenk@u.washington.edu.
*E-mail: ajen@u.washington.edu.

Present Addresses

[▽]Institute of Photovoltaics, 999 Xuefu Avenue, Nanchang 330031, China.
[⊥]Department of Natural and Applied Sciences, University of Wisconsin-Green Bay, Green Bay, WI, 94311.
[¶]Department of Polymer Science and Engineering, Zhejiang University, Hangzhou 310027, China.

Author Contributions

[§]These authors contributed equally to this work.

Notes

The authors declare no competing financial interest.

ACKNOWLEDGMENTS

This paper is based on work supported by the Office of Naval Research (thin film spectroscopy and analysis by D.B.S., C.W.S. and D.S.G., materials development and characterization by K.Y., J.I., S.W., C.Z.L., C.C.C., and A.K.Y.J., N00014-14-1-0170). D.B.S. is supported by the National Science Foundation Graduate Research Fellowship Program (2013118402). C.W.S. acknowledges partial support from the US NSF SEES fellowship program (analysis, DMR-1215753). The GIWAXS component of this work was supported by the Department of Energy Office of Basic Energy Sciences under award number DE-SC0005153 (by J.R., Y.X., and L.D.P.).

REFERENCES

(1) He, Z. C.; Zhong, C. M.; Su, S. J.; Xu, M.; Wu, H. B.; Cao, Y. Enhanced power-conversion efficiency in polymer solar cells using an inverted device structure. *Nat. Photonics* **2012**, *6*, 591.
(2) Zhang, S. Q.; Ye, L.; Zhao, W. C.; Liu, D. L.; Yao, H. F.; Hou, J. H. Side Chain Selection for Designing Highly Efficient Photovoltaic Polymers with 2D-Conjugated Structure. *Macromolecules* **2014**, *47*, 4653.
(3) Ye, L.; Zhang, S. Q.; Zhao, W. C.; Yao, H. F.; Hou, J. H. Highly Efficient 2D-Conjugated Benzodithiophene-Based Photovoltaic Polymer with Linear Alkylthio Side Chain. *Chem. Mater.* **2014**, *26*, 3603.
(4) You, J. B.; Dou, L. T.; Yoshimura, K.; Kato, T.; Ohya, K.; Moriarty, T.; Emery, K.; Chen, C. C.; Gao, J.; Li, G.; Yang, Y. A polymer tandem solar cell with 10.6% power conversion efficiency. *Nat. Commun.* **2013**, *4*, 1446.
(5) Giebink, N. C.; Wiederrecht, G. P.; Wasielewski, M. R.; Forrest, S. R. Thermodynamic efficiency limit of excitonic solar cells. *Phys. Rev. B: Condens. Matter Mater. Phys.* **2011**, *83*, 195326.
(6) Scharber, M. C.; Sariciftci, N. S. Efficiency of bulk-heterojunction organic solar cells. *Prog. Polym. Sci.* **2013**, *38*, 1929.
(7) Servaites, J. D.; Ratner, M. A.; Marksb, T. J. Practical efficiency limits in organic photovoltaic cells: Functional dependence of fill

DOI: 10.1021/acs.chemmater.5b02133
Chem. Mater. 2015, 27, 6583−6591

factor and external quantum efficiency. *Appl. Phys. Lett.* **2009**, *95*, 163302.
(8) Zhang, G. Y.; Huber, R. C.; Ferreira, A. S.; Boyd, S. D.; Luscombe, C. K.; Tolbert, S. H.; Schwartz, B. J. Crystallinity Effects in Sequentially Processed and Blend-Cast Bulk-Heterojunction Polymer/Fullerene Photovoltaics. *J. Phys. Chem. C* **2014**, *118*, 18424.
(9) Hedley, G. J.; Ward, A. J.; Alekseev, A.; Howells, C. T.; Martins, E. R.; Serrano, L. A.; Cooke, G.; Ruseckas, A.; Samuel, I. D. W. Determining the optimum morphology in high-performance polymer-fullerene organic photovoltaic cells. *Nat. Commun.* **2013**, *4*, 2867.
(10) Yang, B.; Yuan, Y. B.; Huang, J. S. Reduced Bimolecular Charge Recombination Loss in Thermally Annealed Bilayer Heterojunction Photovoltaic Devices with Large External Quantum Efficiency and Fill Factor. *J. Phys. Chem. C* **2014**, *118*, 5196.
(11) Rao, A.; Chow, P. C. Y.; Gelinas, S.; Schlenker, C. W.; Li, C. Z.; Yip, H. L.; Jen, A. K. Y.; Ginger, D. S.; Friend, R. H. The role of spin in the kinetic control of recombination in organic photovoltaics. *Nature* **2013**, *500*, 435.
(12) Burke, T. M.; Sweetnam, S.; Vandewal, K.; McGehee, M. D. Beyond Langevin Recombination: How Equilibrium Between Free Carriers and Charge Transfer States Determines the Open-Circuit Voltage of Organic Solar Cells. *Adv. Energy Mater.* **2015**, *5*, 1500123.
(13) Knesting, K. M.; Ju, H. X.; Schlenker, C. W.; Giordano, A. J.; Garcia, A.; Smith, O. L.; Olson, D. C.; Marder, S. R.; Ginger, D. S. ITO Interface Modifiers Can Improve V-OC in Polymer Solar Cells and Suppress Surface Recombination. *J. Phys. Chem. Lett.* **2013**, *4*, 4038.
(14) Shao, G.; Glaz, M. S.; Ma, F.; Ju, H.; Ginger, D. S. Intensity-modulated scanning Kelvin probe microscopy for probing recombination in organic photovoltaics. *ACS Nano* **2014**, *8*, 10799.
(15) Chen, L. M.; Xu, Z.; Hong, Z. R.; Yang, Y. Interface investigation and engineering - achieving high performance polymer photovoltaic devices. *J. Mater. Chem.* **2010**, *20*, 2575.
(16) Vandewal, K.; Albrecht, S.; Hoke, E. T.; Graham, K. R.; Widmer, J.; Douglas, J. D.; Schubert, M.; Mateker, W. R.; Bloking, J. T.; Burkhard, G. F.; Sellinger, A.; Frechet, J. M. J.; Amassian, A.; Riede, M. K.; McGehee, M. D.; Neher, D.; Salleo, A. Efficient charge generation by relaxed charge-transfer states at organic interfaces. *Nat. Mater.* **2014**, *13*, 63.
(17) Vandewal, K.; Tvingstedt, K.; Gadisa, A.; Inganas, O.; Manca, J. V. Relating the open-circuit voltage to interface molecular properties of donor:acceptor bulk heterojunction solar cells. *Phys. Rev. B: Condens. Matter Mater. Phys.* **2010**, *81*, 125204.
(18) Vandewal, K.; Tvingstedt, K.; Inganas, O. Polarization anisotropy of charge transfer absorption and emission of aligned polymer: fullerene blend films. *Phys. Rev. B: Condens. Matter Mater. Phys.* **2012**, *86*, 035212.
(19) Tvingstedt, K.; Vandewal, K.; Gadisa, A.; Zhang, F. L.; Manca, J.; Inganas, O. Electroluminescence from Charge Transfer States in Polymer Solar Cells. *J. Am. Chem. Soc.* **2009**, *131*, 11819.
(20) Deibel, C.; Strobel, T.; Dyakonov, V. Role of the Charge Transfer State in Organic Donor-Acceptor Solar Cells. *Adv. Mater.* **2010**, *22*, 4097.
(21) Provencher, F.; Berube, N.; Parker, A. W.; Greetham, G. M.; Towrie, M.; Hellmann, C.; Cote, M.; Stingelin, N.; Silva, C.; Hayes, S. C. Direct observation of ultrafast long-range charge separation at polymer-fullerene heterojunctions. *Nat. Commun.* **2014**, *5*, 4288.
(22) Bakulin, A. A.; Rao, A.; Pavelyev, V. G.; van Loosdrecht, P. H. M.; Pshenichnikov, M. S.; Niedzialek, D.; Cornil, J.; Beljonne, D.; Friend, R. H. The Role of Driving Energy and Delocalized States for Charge Separation in Organic Semiconductors. *Science* **2012**, *335*, 1340.
(23) Lee, J.; Vandewal, K.; Yost, S. R.; Bahlke, M. E.; Goris, L.; Baldo, M. A.; Manca, J. V.; Van Voorhis, T. Charge Transfer State Versus Hot Exciton Dissociation in Polymer-Fullerene Blended Solar Cells. *J. Am. Chem. Soc.* **2010**, *132*, 11878.
(24) Piersimoni, F.; Chambon, S.; Vandewal, K.; Mens, R.; Boonen, T.; Gadisa, A.; Izquierdo, M.; Filippone, S.; Ruttens, B.; D'Haen, J.; Martin, N.; Lutsen, L.; Vanderzande, D.; Adriaensens, P.; Manca, J. V. Influence of Fullerene Ordering on the Energy of the Charge-Transfer State and Open-Circuit Voltage in Polymer:Fullerene Solar Cells. *J. Phys. Chem. C* **2011**, *115*, 10873.
(25) Vandewal, K.; Gadisa, A.; Oosterbaan, W. D.; Bertho, S.; Banishoeib, F.; Van Severen, I.; Lutsen, L.; Cleij, T. J.; Vanderzande, D.; Manca, J. V. The relation between open-circuit voltage and the onset of photocurrent generation by charge-transfer absorption in polymer: Fullerene bulk heterojunction solar cells. *Adv. Funct. Mater.* **2008**, *18*, 2064.
(26) Graham, K. R.; Erwin, P.; Nordlund, D.; Vandewal, K.; Li, R. P.; Ndjawa, G. O. N.; Hoke, E. T.; Salleo, A.; Thompson, M. E.; McGehee, M. D.; Amassian, A. Re-evaluating the Role of Sterics and Electronic Coupling in Determining the Open-Circuit Voltage of Organic Solar Cells. *Adv. Mater.* **2013**, *25*, 6076.
(27) Perez, M. D.; Borek, C.; Forrest, S. R.; Thompson, M. E. Molecular and Morphological Influences on the Open Circuit Voltages of Organic Photovoltaic Devices. *J. Am. Chem. Soc.* **2009**, *131*, 9281.
(28) Ripolles-Sanchis, T.; Raga, S. R.; Guerrero, A.; Welker, M.; Turbiez, M.; Bisquert, J.; Garcia-Belmonte, G. Molecular Electronic Coupling Controls Charge Recombination Kinetics in Organic Solar Cells of Low Bandgap Diketopyrrolopyrrole, Carbazole, and Thiophene Polymers. *J. Phys. Chem. C* **2013**, *117*, 8719.
(29) Vandewal, K.; Widmer, J.; Heumueller, T.; Brabec, C. J.; McGehee, M. D.; Leo, K.; Riede, M.; Salleo, A. Increased open-circuit voltage of organic solar cells by reduced donor-acceptor interface area. *Adv. Mater.* **2014**, *26*, 3839.
(30) Zhang, Y.; Zou, J. Y.; Yip, H. L.; Chen, K. S.; Zeigler, D. F.; Sun, Y.; Jen, A. K. Y. Indacenodithiophene and Quinoxaline-Based Conjugated Polymers for Highly Efficient Polymer Solar Cells. *Chem. Mater.* **2011**, *23*, 2289.
(31) Heeney, M.; Zhang, W.; Crouch, D. J.; Chabinyc, M. L.; Gordeyev, S.; Hamilton, R.; Higgins, S. J.; McCulloch, I.; Skabara, P. J.; Sparrowe, D.; Tierney, S. Regioregular poly(3-hexyl) selenophene: a low band gap organic hole transporting polymer. *Chem. Commun.* **2007**, 5061.
(32) Vandewal, K.; Tvingstedt, K.; Gadisa, A.; Inganas, O.; Manca, J. V. On the origin of the open-circuit voltage of polymer-fullerene solar cells. *Nat. Mater.* **2009**, *8*, 904.
(33) Hoke, E. T.; Vandewal, K.; Bartelt, J. A.; Mateker, W. R.; Douglas, J. D.; Noriega, R.; Graham, K. R.; Frechet, J. M. J.; Salleo, A.; McGehee, M. D. Recombination in Polymer:Fullerene Solar Cells with Open-Circuit Voltages Approaching and Exceeding 1.0 V. *Adv. Energy Mater.* **2013**, *3*, 220.
(34) Bernardo, B.; Cheyns, D.; Verreet, B.; Schaller, R. D.; Rand, B. P.; Giebink, N. C. Delocalization and dielectric screening of charge transfer states in organic photovoltaic cells. *Nat. Commun.* **2014**, *5*, 3245.
(35) Marcus, R. A. Relation between Charge-Transfer Absorption and Fluorescence-Spectra and the Inverted Region. *J. Phys. Chem.* **1989**, *93*, 3078.
(36) Gould, I. R.; Noukakis, D.; Gomez-Jahn, L.; Young, R. H.; Goodman, J. L.; Farid, S. Radiative and Nonradiative Electron-Transfer in Contact Radical-Ion Pairs. *Chem. Phys.* **1993**, *176*, 439.
(37) Street, R. A.; Krakaris, A.; Cowan, S. R. Recombination Through Different Types of Localized States in Organic Solar Cells. *Adv. Funct. Mater.* **2012**, *22*, 4608.
(38) Street, R. A.; Khlyabich, P. P.; Rudenko, A. E.; Thompson, B. C. Electronic States in Dilute Ternary Blend Organic Bulk Heterojunction Solar Cells. *J. Phys. Chem. C* **2014**, *118*, 26569.
(39) Blakesley, J. C.; Neher, D. Relationship between energetic disorder and open-circuit voltage in bulk heterojunction organic solar cells. *Phys. Rev. B: Condens. Matter Mater. Phys.* **2011**, *84*, 075210.
(40) Lee, C. C.; Su, W. C.; Chang, W. C.; Huang, B. Y.; Liu, S. W. The effect of charge transfer state on open-circuit voltage of small-molecular organic photovoltaic devices: A comparison between the planar and bulk heterojunction using electroluminescence characterization. *Org. Electron.* **2015**, *16*, 1.
(41) Sutton, C.; Sears, J. S.; Coropceanu, V.; Bredas, J. L. Understanding the Density Functional Dependence of DFT-

DOI: 10.1021/acs.chemmater.5b02133
Chem. Mater. 2015, 27, 6583−6591

Calculated Electronic Couplings in Organic Semiconductors. *J. Phys. Chem. Lett.* **2013**, *4*, 919.
(42) Kawatsu, T.; Coropceanu, V.; Ye, A. J.; Bredas, J. L. Quantum-chemical approach to electronic coupling: Application to charge separation and charge recombination pathways in a model molecular donor-acceptor system for organic solar cells. *J. Phys. Chem. C* **2008**, *112*, 3429.
(43) Liu, T.; Troisi, A. Absolute Rate of Charge Separation and Recombination in a Molecular Model of the P3HT/PCBM Interface. *J. Phys. Chem. C* **2011**, *115*, 2406.
(44) Jarzab, D.; Cordella, F.; Gao, J.; Scharber, M.; Egelhaaf, H. J.; Loi, M. A. Low-Temperature Behaviour of Charge Transfer Excitons in Narrow-Bandgap Polymer-Based Bulk Heterojunctions. *Adv. Energy Mater.* **2011**, *1*, 604.
(45) Loi, M. A.; Toffanin, S.; Muccini, M.; Forster, M.; Scherf, U.; Scharber, M. Charge transfer excitons in bulk heterojunctions of a polyfluorene copolymer and a fullerene derivative. *Adv. Funct. Mater.* **2007**, *17*, 2111.
(46) Di Nuzzo, D.; Wetzelaer, G. J. A. H.; Bouwer, R. K. M.; Gevaerts, V. S.; Meskers, S. C. J.; Hummelen, J. C.; Blom, P. W. M.; Janssen, R. A. J. Simultaneous Open-Circuit Voltage Enhancement and Short-Circuit Current Loss in Polymer: Fullerene Solar Cells Correlated by Reduced Quantum Efficiency for Photoinduced Electron Transfer. *Adv. Energy Mater.* **2013**, *3*, 85.
(47) Tedlla, B. Z.; Zhu, F.; Cox, M.; Drijkoningen, J.; Manca, J.; Koopmans, B.; Goovaerts, E. Understanding Triplet Formation Pathways in Bulk Heterojunction Polymer:fullerene Photovoltaic Devices. *Adv. Energy Mater.* **2015**, *5*, 1401109.
(48) Kittel, C. *Introduction to Solid State Physics*, 6th ed.; John Wiley & Sons, Inc.: 1986; p 127.
(49) Orapunt, F.; O'Leary, S. K. Optical transitions and the mobility edge in amorphous semiconductors: A joint density of states analysis. *J. Appl. Phys.* **2008**, *104*, 073513.
(50) Loper, P.; Muller, R.; Hiller, D.; Barthel, T.; Malguth, E.; Janz, S.; Goldschmidt, J. C.; Hermle, M.; Zacharias, M. Quasi-Fermi-level splitting in ideal silicon nanocrystal superlattices. *Phys. Rev. B: Condens. Matter Mater. Phys.* **2011**, *84*, 195317.
(51) Jiang, C. W.; Green, M. A. Silicon quantum dot superlattices: Modeling of energy bands, densities of states, and mobilities for silicon tandem solar cell applications. *J. Appl. Phys.* **2006**, *99*, 114902.
(52) Miller, N. C.; Cho, E.; Junk, M. J. N.; Gysel, R.; Risko, C.; Kim, D.; Sweetnam, S.; Miller, C. E.; Richter, L. J.; Kline, R. J.; Heeney, M.; McCulloch, I.; Amassian, A.; Acevedo-Feliz, D.; Knox, C.; Hansen, M. R.; Dudenko, D.; Chmelka, B. F.; Toney, M. F.; Bredas, J. L.; McGehee, M. D. Use of X-Ray Diffraction, Molecular Simulations, and Spectroscopy to Determine the Molecular Packing in a Polymer-Fullerene Bimolecular Crystal. *Adv. Mater.* **2012**, *24*, 6071.
(53) Mayer, A. C.; Toney, M. F.; Scully, S. R.; Rivnay, J.; Brabec, C. J.; Scharber, M.; Koppe, M.; Heeney, M.; McCulloch, I.; McGehee, M. D. Bimolecular Crystals of Fullerenes in Conjugated Polymers and the Implications of Molecular Mixing for Solar Cells. *Adv. Funct. Mater.* **2009**, *19*, 1173.
(54) Scarongella, M.; Paraecattil, A. A.; Buchaca-Domingo, E.; Douglas, J. D.; Beaupre, S.; McCarthy-Ward, T.; Heeney, M.; Moser, J. E.; Leclerc, M.; Frechet, J. M. J.; Stingelin, N.; Banerji, N. The influence of microstructure on charge separation dynamics in organic bulk heterojunction materials for solar cell applications. *J. Mater. Chem. A* **2014**, *2*, 6218.
(55) Liao, H. C.; Tsao, C. S.; Shao, Y. T.; Chang, S. Y.; Huang, Y. C.; Chuang, C. M.; Lin, T. H.; Chen, C. Y.; Su, C. J.; Jeng, U. S.; Chen, Y. F.; Su, W. F. Bi-hierarchical nanostructures of donor-acceptor copolymer and fullerene for high efficient bulk heterojunction solar cells. *Energy Environ. Sci.* **2013**, *6*, 1938.

DOI: 10.1021/acs.chemmater.5b02133
Chem. Mater. 2015, 27, 6583−6591